Polymer Chemistry

Accepted Manuscript

ROYAL SOCIETY OF CHEMISTRY

www.rsc.org/polymers

Polymer Chemistry

RSCPublishing

ARTICLE

Cite this: DOI: 10.1039/x0xx00000x

Combining the incompatible: Block copolymers consecutively displaying activated esters and amines and their use as protein-repellent surface modifiers with multivalent biorecognition

Daniel Hönders, Thomas Tigges and Andreas Walther*

Received 00th January 2012,
Accepted 00th January 2012

DOI: 10.1039/x0xx00000x

www.rsc.org/

We present the facile synthesis and orthogonal functionalization of diblock copolymers containing two mutually incompatible segments, i.e. primary amines and activated esters, that are displayed chronologically and synthesized by consecutive radical addition fragmentation transfer polymerization (RAFT) of suitably modified monomers. Post-polymerization modification of the active ester moieties with functionalized triethylene glycol derivatives (NH_2-TEG/NH_2-TEG-biotin) furnishes a protein-repellent block with specific biorecognition, and the activation of the amine groups via deprotection results in newly reactive primary amines. We subsequently use these amines as anchoring layer for the coating of aldehyde-functionalized polystyrene (PS) colloids and demonstrate tight adhesion and enhanced protein-repellent characteristics combined with specific and multivalent biorecognition of avidin as a function of block ratios. Our strategy demonstrates a viable approach for orthogonal combination of widely needed, but mutually incompatible, functional groups into complex polymer architectures.

Introduction

The advent of modular ligation based on orthogonal and highly efficient chemical reactions has undoubtedly revolutionized the field of macromolecular engineering.[1-4] Large efforts have been focused on expanding the types of reactions, starting from classical Cu(I)-catalyzed Huisgen cycloaddition of alkynes and azides,[5-21] to thiol-ene chemistry,[22-31] activated esters,[32-40] oxime-click,[41-43] Michael addition[44-47] and hetero Diels-Alder reactions.[48-57] These advances in efficient ligation chemistry are nowadays intensely exploited to make new polymer topologies by clicking separate, functionalized polymeric building blocks instead of step-wise synthesis, or for the efficient post-functionalization of polymers carrying reactive side or end groups. The latter has been developed to a high extent for polymers bearing active ester moieties, which are obtained by controlled radical polymerization of functional monomers into different polymer topologies and subsequently readily modified by nucleophilic substituents.[2, 33, 35]

However, one has to realize that a straightforward application of modular ligation reactions to problems in materials or bio science is limited by the commercial availability of suitably functionalized molecules for sensing, surface immobilization or selective recognition and supramolecular interactions.[58-60] Probably the most widely available and most heavily used types of interactions are still the amine/active ester and the thiol/maleimide pairs, which were classically developed as precision tools in biochemistry.[34, 36, 56, 61]

Herein, we will demonstrate the rather unusual combination of two mutually incompatible units and integrate amines and activated ester functionalities in block copolymers by a two-step radical addition fragmentation transfer polymerization (RAFT) of suitably functionalized monomers. We use a protected amine monomer to prevent immediate coupling reactions during the synthesis, yielding well-defined diblock copolymers. We show that both functionalities can be selectively and sequentially addressed by first modifying the block bearing the activated ester functionalities with functional amines. We use triethylene glycol amine (TEG-NH_2) to prepare branched non-fouling, protein-repellent structures and toward functionalities we incorporate biotinTEG-NH_2 units to allow for selective biorecognition of streptavidin. Afterwards, the protective groups of the protected amines can be removed and we use the newly available amine groups to graft the block copolymers covalently onto aldehyde-functionalized polystyrene (PS) colloids via reductive amination, rendering multivalent specific biorecognition properties in an otherwise protein-repellent layer. The grafted surface layers exhibit increased protein repellency compared to linear polyethylene glycol (PEG) chains and compositionally similar random

*DWI – Leibniz-Institute for Interactive Materials, Forckenbeckstraße 50, 52074 Aachen, Germany. walther@dwi.rwth-aachen.de

copolymers, as well as selective addressability with dye-labeled NeutrAvidin (NAv) once the biotin tags are incorporated.

Experimental

Starting materials, instrumentation, monomer synthesis and synthesis of triethylene glycol amine (TEG-NH_2), biotin-4,7,10-trioxa-13-tridecaneamine (BiotinTEG-NH_2) and random copolymers can be found in the Supplementary Information.

Synthesis of diblock copolymers

Synthesis of poly(*t*-Boc-aminoethyl acrylate) (PBocAEA) by RAFT polymerization

t-Boc-aminoethyl acrylate (BocAEA) (6.89 g, 32.02 mmol, 40 eq) and 2-(dodecylthiocarbonothioylthio)-2-methylpropanoic acid (DDMAT) (0.29 g, 0.80 mmol) were dissolved in 13.8 mL anhydrous *N*,*N*-dimethylformamide (DMF) and the solution was deoxygenated by bubbling with nitrogen for 30 min. In a second vessel, a stock solution of azobisisobutyronitrile (AIBN) (0.19 mmol) in DMF (2 mL) was degassed similarly. After degassing, the monomer mixture was placed in a preheated oil bath at 70 °C, and subsequently 0.27 mL (0.02 mmol, 0.02 eq) of degassed AIBN stock solution was introduced into the reaction mixture in a ratio of [M]:[CTA]:[AIBN] = 40/1/0.02 (example). The polymerization was conducted under nitrogen atmosphere and samples for nuclear magnetic resonance (NMR) spectroscopy and size-exclusion chromatography (SEC) analysis were withdrawn to monitor conversion and obtain PBocAEA of desired length. After certain reaction time, the reaction was stopped by freezing the reaction vessel in liquid nitrogen. Polymers were isolated from the reaction mixture via dilution with dioxane and subsequently precipitated in cold hexane. Precipitations from dioxane into hexane was repeated twice before the polymer was freeze-dried from dioxane yielding a yellowish polymer.
^{1}H NMR ($CDCl_3$, 400 MHz): δ/ppm: 5.66 (br, $-CH_2$-N**H**-Boc), 4.12 (br, -O-C**H_2**-CH_2-), 3.34 (br, -CH_2-C**H_2**-NH-), 2.50-1.57 (br, backbone -C**H_2**-C**H**-), 1.42 (br, -NH-**Boc**), 1.30-1.20 (br, -SC(S)S-CH_2-(C**H_2**)$_{10}$-CH_3), 0.86 (t, -SC(S)S-CH_2-$(CH_2)_{10}$-C**H_3**). **^{13}C NMR ($CDCl_3$, 100 MHz):** δ/ppm: 174.5, 156.0, 79.2, 63.9, 41.6, 39.4, 35.0, 31.8, 29.5, 29.4, 29.3, 29.2, 29.0, 28.4, 22.6, 14.0.

Synthesis of poly(*t*-Boc-aminoethyl acrylate)-*block*-poly(pentafluorophenyl acrylate) (PBocAEA-*b*-PPFPA)

In a typical experiment, 1.36 g PBocAEA ($M_{n,calc}$ = 5,700 g/mol, 0.24 mmol) and 5.12 g pentafluorophenyl acrylate (PFPA) (21.51 mmol) was mixed in 13 mL anhydrous dioxane and the mixture was degassed by three freeze-thaw evacuation cycles. The reaction vessel was placed in a preheated oil bath at 70 °C and 0.24 mL of a degassed stock solution of AIBN (0.13 mmol in 2 mL dioxane) was subsequently injected in a ratio of [M]:[macro-CTA]:[AIBN] = 92/1/0.07 (example).
The polymerization was conducted under nitrogen atmosphere and samples for NMR and SEC analysis were withdrawn to monitor conversion and obtain PBocAEA-*b*-PPFPA diblock copolymer of desired compositions. After certain reaction time, the reaction was stopped by freezing the vessel in liquid nitrogen. Precipitation from dioxane into hexane/diethyl ether mixture (3:1) was repeated twice to remove any remaining PBocAEA before the polymer was freeze-dried from dioxane yielding a yellow solid polymer.
^{1}H NMR ($CDCl_3$, 400 MHz): δ/ppm: 5.66 (br, $-CH_2$-N**H**-Boc), 4.12 (br, -O-C**H_2**-CH_2-), 3.34 (br, -CH_2-C**H_2**-NH-), 3.08 (br, backbone -CH_2-C**H**-(PFPA)) 2.50-1.57 (br, backbone -C**H_2**-C**H**-), 1.42 (br, -NH-**Boc**), 1.30-1.20 (br, -SC(S)S-CH_2-(C**H_2**)$_{10}$-CH_3), 0.86 (t, -SC(S)S-CH_2-$(CH_2)_{10}$-C**H_3**). **^{13}C NMR ($CDCl_3$, 100 MHz):** δ/ppm: 174.5, 170.1, 156.0, 142.7, 141.2, 139.8, 139.3, 138.7, 136.8, 124.5, 79.2, 63.9, 41.6, 39.4, 35.0, 31.8, 29.5, 29.4, 29.3, 29.2, 29.0, 28.4, 22.6, 14.0. **^{19}F NMR ($CDCl_3$, 376 MHz):** δ/ppm: -162.3, -156.9, -153.2.

Post-polymerization modification

Post-polymerization modification of PBocAEA-*b*-PPFPA

In a typical experiment, PBocAEA25-*b*-PPFPA33 ($M_{n,calc}$ = $M_{n,calc}$ =13,600 g/mol, 0.6 g, 1.46 mmol in PFPA moieties) was dissolved in anhydrous DMF (3 mL) and the solution was purged with nitrogen. BiotinTEG-NH_2 (33 mg, 0.073 mmol, 0.05 eq) in 2 mL DMF and triethylamine (TEA) (8 mg, 0.08 mmol) was added to this solution. The mixture was stirred for 24 h under a nitrogen atmosphere at room temperature. Afterward, an excess of TEG-NH_2 (0.34 g, 2.18 mmol, 1.5 eq) was added together with TEA (0.22 g, 2.18 mmol). The mixture was stirred for additional 24 h at room temperature to ensure complete conversion of all active ester groups (monitored by ^{19}F NMR). The solution was concentrated *in vacuo,* precipitated three times in a hexane/diethyl ether mixture (7:3) and freeze-dried from dioxane yielding a yellow highly viscous polymer. Diblock copolymers without biotin function were prepared in an analogous way by post-functionalization of PBocAEA-*b*-PPFPA with a slight excess of TEG-NH_2 and omitting biotinTEG-NH_2.

Deprotection of poly(*t*-Boc-aminoethyl acrylate)-*block*-poly((triethylene glycol acrylamide)-*co*-poly(biotin-4,7,10-trioxa-13-tridecane acrylamide)) (PBocAEA-*b*-P(TEGA-*co*-BiotinTEGA)) and PBocAEA-*b*-P(TEGA)

The *t*-Boc-protected diblock copolymer (100-200 mg) was dissolved in dichloromethane (DCM) (2.5 mL) and the solution was cooled to 0 °C while it was purged with nitrogen. trifluoroacetic acid (TFA) (2.5 mL) was added dropwise to the cooled solution and the reaction mixture was stirred for 4 h at room temperature. After DCM and TFA were removed by evaporation, the oily residue was dissolved in dioxane and precipitated three times in diethyl ether. The resultant precipitate was collected by centrifugation and lyophilized to give a highly viscous polymeric liquid.

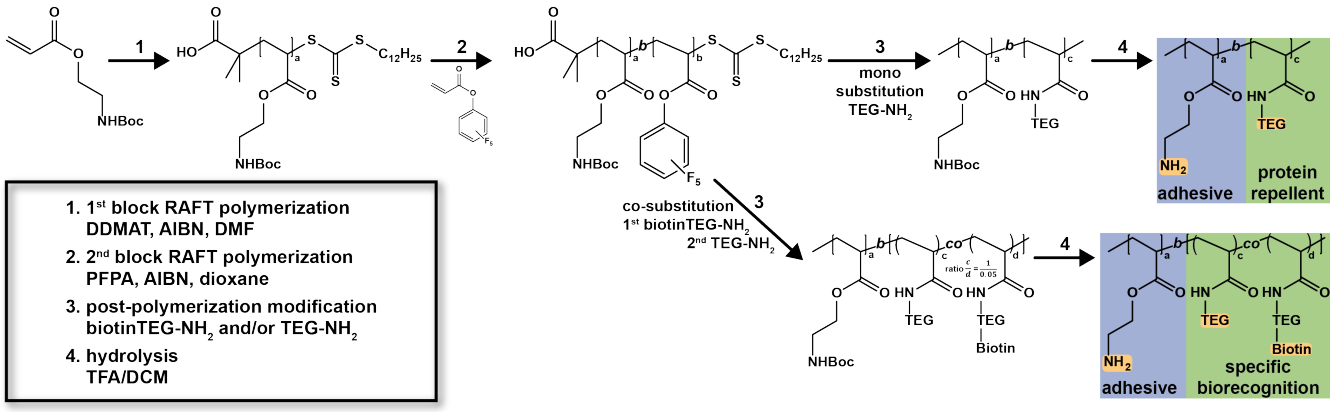

Scheme 1 RAFT synthesis of tailor-made diblock copolymers bearing protected amine and activated ester functionalities and their subsequent activation and modification with side chains for protein repellency and multivalent specific biorecognition. The preparation of the diblock copolymer starts with RAFT polymerization of BocAEA using DDMAT as CTA, followed by chain extension with PFPA. Substitution of the PFPA moieties with TEG-NH_2 and/or biotin-TEG-NH_2 and subsequent acidic deprotection leads to two diblock copolymers which differ in biorecognition and protein repellency, whereas the amine block bears the adhesive segment for immobilization onto various surfaces.

Homogeneous coating of polystyrene microspheres

50 µL of polystyrene (PS) beads with aldehyde/sulfate (4% w/v in ethanol) were added to a solution of PBocAEA-*b*-P(TEGA-*co*-BiotinTEGA) (100 µL, 51 g/L in methanol), or PBocAEA-*b*-P(TEGA) (100 µL, 51 g/L in methanol) or pure methanol (100 µL), respectively. All suspensions were filled with methanol to 1 mL and vortexed for 24 h at rt. Afterwards a solution of $NaCNBH_3$ (50 µL, 10 g/L in methanol) was added to each sample and vortexing was continued for additional 24 h. The microspheres were then separated by centrifugation and washed three times with ethanol, twice with NaCl solution (500 mM in water) to break interpolyelectrolyte complexes and twice with phosphate-buffered saline solution (PBS) buffer (pH 7.4).

Binding of fluorescent avidin conjugate to microspheres

500 µL of microsphere suspension (2 g/L) in PBS-solution either coated with PBocAEA-*b*-P(TEGA-*co*-BiotinTEGA), PBocAEA-*b*-P(TEGA) or uncoated were incubated with 25 µL of an Oregon Green 488 conjugate of NAv biotin-binding protein (1 g/L) for 10 min under shaking and protection from light. The microspheres were then separated by centrifugation, washed three times with PBS and finally resuspended in 100 µL of PBS. The binding of fluorescent avidin to microparticles was investigated and visualized by confocal laser scanning microscopy ($\lambda_{ex} = 488$ nm) and the unbound fraction of labeled NAv was characterized by fluorescence spectroscopy of the supernatant. For each set of samples, the same detector settings were chosen.

Results and discussion

The general synthetic strategy commences with the RAFT polymerization of a *t*-Boc protected aminoethyl acrylate (BocAEA), using 2-(dodecylthiocarbonothioylthio)-2-methylpropionic acid (DDMAT) as a chain transfer agent (CTA) and azobisisobutyronitril (AIBN) as radical source (Scheme 1). The corresponding deprotected polymer has recently attracted interest for its ability to complex DNA for efficient gene delivery,[62-66] yet controlled polymerization procedures are scarcely reported and mostly focus on *t*-Boc protected aminoethyl methacrylate (BocAEMA) and atom transfer radical addition (ATRP).[62-65, 67, 68] RAFT polymerization of BocAEA has recently first been described[66], but sequential block copolymerization of vinyl monomers and complex polymer architectures still need to be shown to unravel the potential of this attractive monomer. Next, the first block is chain extended using pentafluorophenyl acrylate (PFPA), which is a well understood building block for polymers bearing activated ester units.[69] Subsequently, we selectively and orthogonally address both functionalities using substitution of the activated ester groups by primary and functional triethylene glycol amine (TEG-NH_2) and small amounts of biotin-4,7,10-trioxa-13-tridecaneamine (BiotinTEG-NH_2), followed by acidic deprotection of the *t*-Boc groups.

Since we focus on the application of the targeted diblock copolymers as multivalent surface modifiers for the controlled functionalization of colloidal particles with high grafting density, we target diblock copolymers with relatively low molecular weights and relatively small fractions of the final adhesive block (PBocAEA). Figure 1a-c summarizes the representative results of the RAFT mediated polymerization kinetics of BocAEA. The first order kinetic plot of the polymerization of BocAEA ($[BocAEA]_0:[CTA]_0:[AIBN]_0 = 40:1:0.04$) displays a linear relationship, being indicative of a constant radical concentration and a controlled radical polymerization (Figure 1a). The corresponding elution traces in size exclusion chromatography (SEC) reveal a consistent shift toward lower elution volumes with increasing conversion and low dispersity ($Đ$) smaller 1.18 (Figure 1b,c). The thus far developed synthetic protocol allows the facile preparation of PBocAEA homopolymers with

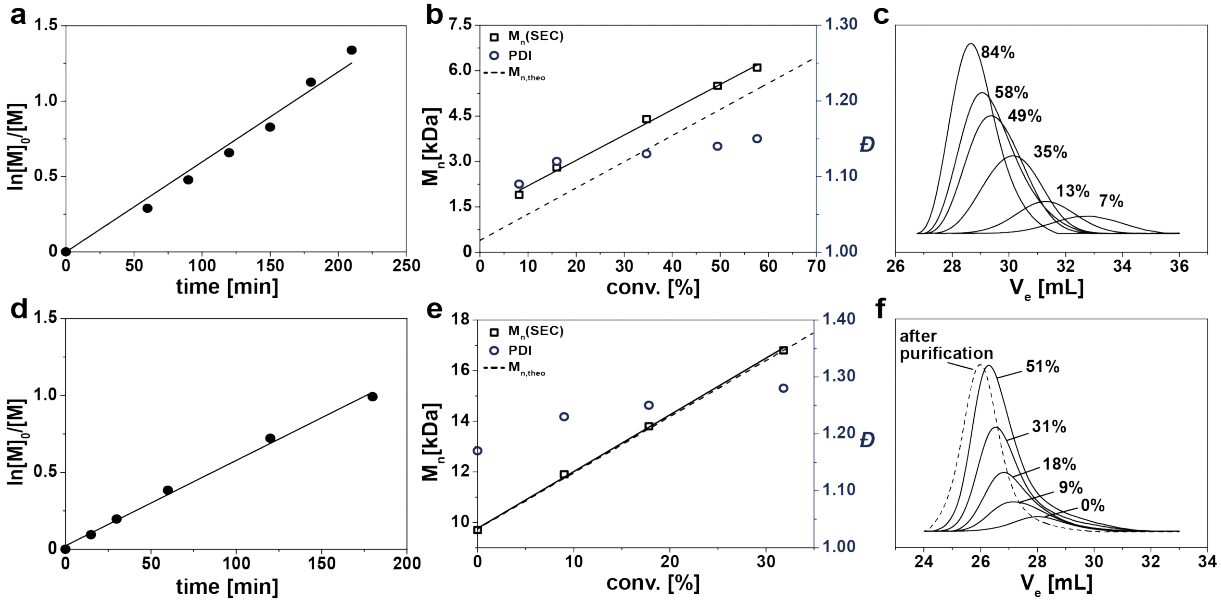

Figure 1 RAFT polymerization kinetics for the diblock copolymer synthesis. Synthesis of PBocAEA: (a) First order kinetic plot, **(b)** evolution of molecular weights and dispersities as a function of conversion and **(c)** SEC profiles in THF for the homopolymerization of BocAEA via RAFT polymerization using DDMAT as CTA and AIBN as initiator in the ratio $[BocAEA]_0:[CTA]_0:[AIBN]_0 = 40/1/0.04$ in DMF at 70 °C. **Chain extension toward PBocAEA-*b*-PPFPA: (d)** First order kinetic plot, **(e)** evolution of molecular weights and dispersities as a function of conversion and **(f)** SEC profiles in THF during reaction and after selective precipitation for the polymerization of PFPA via RAFT polymerization at $[PFPA]_0:[PBocAEA\text{-}CTA]_0:[AIBN]_0 = 130/1/0.07$. Reaction was performed in dioxane at 70 °C.

Table 1. Summary of characterization results of PBocAEA-*b*-PPFPA and two starting PBocAEA-CTA macro chain transfer agents

Polymer [a]	$M_{n,calc}$(Da) [b]	$M_{n,SEC}$ (Da) [c]	Đ
PBocAEA25	5,700	7,100	1.16
PBocAEA25-*b*-PPFPA33	13,600	15,100	1.22
PBocAEA25-*b*-PPFPA60	20,000	18,400	1.26
PBocAEA39	8,800	8,300	1.17
PBocAEA39-*b*-PPFPA88	29,700	19,200	1.29

[a]The numbers behind the individual blocks correspond to the degree of polymerization, as determined by ^{1}H NMR (after precipitation in hexane/diethyl ether). [b]Calculation based on the weight fractions determined by ^{1}H NMR and the true molecular weight of the PBocAEA-CTA determined by end-group analysis using ^{1}H NMR . [c] SEC in THF calibrated with PMMA standards.

molecular weights up to 10,000 Da by varying the ratio of $[BocAEA]_0:[CTA]_0$ up to 100.

The obtained signals in MALDI-ToF mass spectrometry (Figure 2) can clearly be assigned to the proposed RAFT polymer and the peak separation fits to the BocAEA repeating unit (215.25 Da). The two main series correspond to the complexation with Na^+ of NaTFAc and H^+. Other series with low intensities are attributed to slight fragmentation of the end-groups.[70] Each mass obtained for the dominant series can be explained as the sum of n repeating units of $M_{BocAEA} + M_{DDMAT} + M_{Na}$. For instance, we find that the experimental molecular weight for $n = 17$ repeating units ($m/z = 4046$ Da) fits well to the theoretical molecular weight of 4047 Da. Similarly, the exemplary molecular weight of the minor series at $m/z = 4024$ Da corresponds to the protonated molecule and fits to the theoretical weight of 4025 Da.

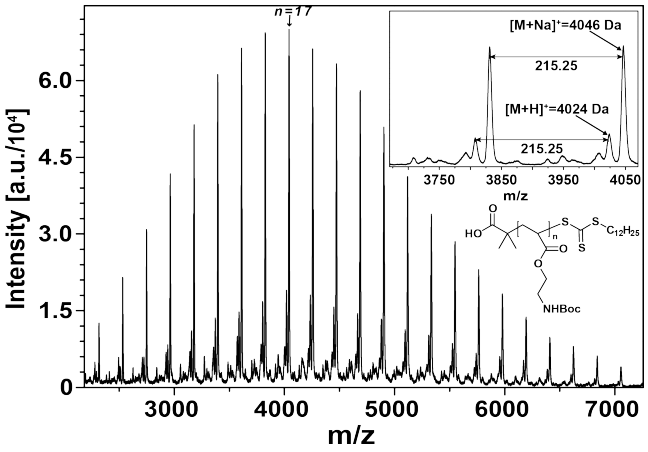

Figure 2 RAFT end-group characterization via MALDI-ToF of a selected PBocAEA-CTA homopolymer.

These two series confirm the incorporation of the CTA and a near complete functionalization of the polymer chain ends and absence of termination products. Importantly, this allows to use ^{1}H NMR end-group analysis to determine the absolute number average molecular weights.

Subsequently, we chain-extended selected PBocAEA homopolymers with PFPA at starting ratios of $[PFPA]_0:[PBocAEA\text{-}CTA]_0:[AIBN]_0 = 130:1:0.07$. The corresponding first order kinetic plots and SEC traces similarly confirm a successful chain extension and a controlled radical polymerization taking place (Figure 1d-f). We tune the length of the second block by conveniently taking samples from a running reaction, allowing to tailor the weight fractions of both blocks. Characterization by SEC shows a distinct shift in

molecular weight toward lower elution volumes with increasing monomer conversion, hence confirming the successful chain extension. The slight broadening of the molecular weight distribution and a slight shoulder at higher elution volumes indicate some incomplete blocking efficiency. Remaining PBocAEA homopolymer can however be efficiently removed by selective precipitation in a solvent mixture of diethyl ether/hexane 1:3 (dotted line in Figure 1f) resulting in various well-defined diblock copolymers with narrow distribution ($Đ \leq 1.3$) for different degrees of polymerization. Table 1 summarizes the molecular weight characterization for two PBocAEA-CTAs and three diblock copolymers used in the following. Interesting differences can be observed when comparing the apparent molecular weights ($M_{n,SEC}$) to the accurate ones, determined by end group analysis and compositional analysis via NMR ($M_{n,calc}$). For short PFPA blocks, we find a higher $M_{n,SEC}$ compared to $M_{n,calc}$, while this relationship inverts for longer PFPA blocks (entry 2 and 3). This difference becomes even more pronounced for longer PFPA blocks (entry 5). We relate this to the differences in hydrodynamic volume and the non-linear dependence of the hydrodynamic volume on composition in such diblock copolymers. In summary, the SEC mainly serves as a valid analytical tool to measure the distribution, while the exact molecular weights can be calculated from NMR with high accuracy for relatively low molecular weight polymers.

Most importantly, the integrity of the *t*-Boc protected groups is confirmed by the absence of crosslinking reactions, which

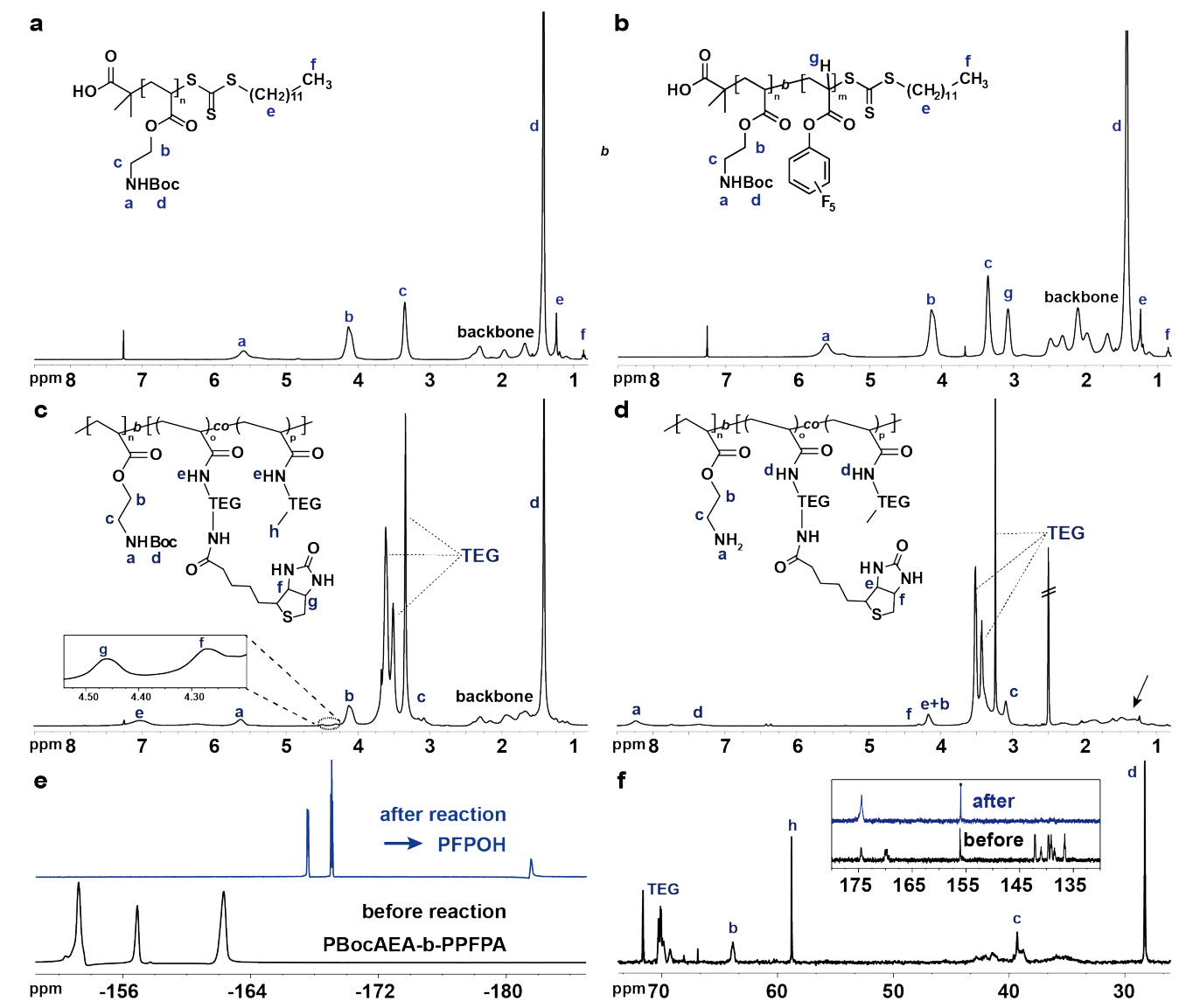

Figure 3 Structural characterization of homo and diblock copolymers before and after modification and hydrolysis using NMR spectroscopy: (a) ^{1}H NMR spectroscopy for PBocAEA homopolymer in $CDCl_3$, **(b)** ^{1}H NMR spectroscopy for PBocAEA-*b*-PPFPA in $CDCl_3$, **(c)** ^{1}H NMR spectroscopy for PBocAEA-*b*-P(TEGA-*co*-BiotinTEGA) in $CDCl_3$ after post-polymerization modification of PBocAEA-*b*-PPFPA, **(d)** ^{1}H NMR spectroscopy for PAEA-*b*-P(TEGA-*co*-BiotinTEGA) in DMSO after deprotection with TFA in DCM, **(e)** ^{19}F NMR spectra for PBocAEA-*b*-PPFPA (bottom) and PBocAEA-*b*-P(TEGA-*co*-BiotinTEGA) (top) in $CDCl_3$ demonstrating quantitative modification of PBocAEA-*b*-PPFPA, **(f)** ^{13}C NMR spectrum for PBocAEA-*b*-P(TEGA-*co*-BiotinTEGA) in $CDCl_3$, inset shows difference at higher chemical shift before and after modification of PBocAEA-*b*-PPFPA.

would be visible at lower elution volumes in the SEC traces or macroscopically as gel formation.

Additional ^{1}H NMR further supports the integrity of the *t*-Boc functionalities and the successful chain extension using PFPA. The persistent protons of the *t*-Boc group are visible at 1.4 ppm for both the homopolymer (PBocAEA-CTA) and the diblock copolymers (PBocAEA-*b*-PPFPA; Figure 3a,b). Due to the fact that PFPA does not contain additional protons in the side chain, its presence and actual fraction can only be concluded from the appearance of further signals in the range of the polyacrylate backbone at 3.1 ppm and the presence of signals in ^{19}F NMR spectroscopy at -162, -157 and -153 ppm (Figure 3e, bottom).

Furthermore, ^{1}H NMR, ^{13}C NMR and ^{19}F NMR provide a viable proof for a quantitative functionalization of the PFPA moieties with functional amines (Figure 3c-f). We demonstrate the successful co-functionalization of TEG-NH_2/Biotin-TEG-NH_2 as a more complex example of post-modification of the diblock copolymers. We use a molar ratio of TEG-NH_2/Biotin-TEG-NH_2 1:0.05 in a sequential co-substitution of the active ester block in a one-pot reaction by initial addition of Biotin-TEG-NH_2 (5 mol% to PFPA groups) followed by addition of a slight excess of TEG-NH_2 to PFPA groups (1.5 equiv). We use biotin as a first example of the possible selective integration of a biorecognition unit in otherwise protein-repellent TEG side chains.

Figure 3c clearly shows the appearance of additional signals in the ^{1}H NMR spectrum (3.1-3.8 ppm) which can be assigned to the newly introduced TEG groups. At the same time, the signals corresponding to the PPFPA backbone at 3.1 and 2.1 ppm disappear. The signal of the amide proton (-N**H**-CO-) of the new linkages appears at 7.0 ppm. Additional small signals at 4.45 and 4.26 ppm (see inset in Figure 3c) originate from the two -C**H**- groups within the biotin units, confirming their successful integration into the diblock copolymer. Analysis of the integrals associated with the new peaks and the signal of the BocAEA side group (4.1 ppm) indicate a quantitative substitution at the active ester moieties and the formation of the TEG-acrylamides. A further comparison of the biotin signals confirms a quantitative incorporation of the targeted 5 mol% Biotin-TEG-NH_2 side chains. Additionally, ^{19}F NMR confirms the full conversion of active ester units by absence of PPFPA signals at -162, -157 and -153 ppm and the appearance of new sharp peaks at lower chemical shifts originating from the released pentafluorophenol (PFPOH, Figure 3e). Furthermore, ^{13}C NMR (Figure 3f) corroborates the successful modification by appearance of new signals at 70 ppm and 59 ppm, arising from the TEG side chains, and disappearance of the distinct PFPA signals at higher chemical shifts (see inset in Figure 3f).

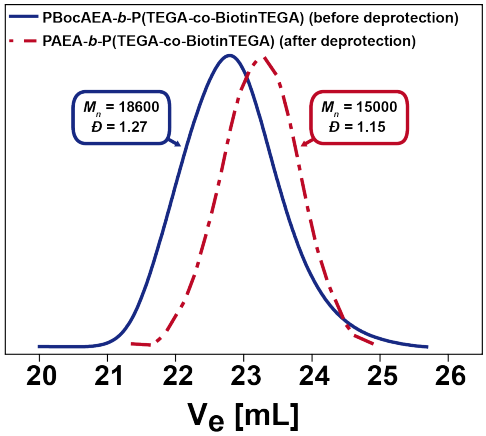

Figure 4 SEC traces of PBocAEA-*b*-P(TEGA-*co*-BiotinTEGA) in DMAc before and after deprotection.

Subsequently, the functionalized diblock copolymers can be activated with respect to the amine functionality by selective acidic deprotection using trifluoroacetic acid (TFA) in dichloromethane (DCM). This step is confirmed by the quantitative disappearance of the strong peak at 1.4 ppm of the *t*-Boc group and the slight shift of the methylene signals in proximity of the newly formed amine group (Figure 3d).

We assured the integrity of the diblock copolymer structure after deprotection by further SEC measurements in dimethylacetamide (DMAc) as eluent (Figure 4). Standard SEC in THF fails due to adsorption of the polymer on the columns. The molecular weight distribution of about 1.15 is narrow and the shift to higher elution volume is expected, as the molecular weight decreases after cleaving the *t*-Boc groups. Furthermore, the unimodal character of the SEC trace at higher elution volume indicates quantitative conversion of all PFPA moieties during the previous modification step since there is no evidence of crosslinked high molecular weight species.

In summary, we established an efficient synthetic strategy to prepare well-defined diblock copolymers incorporating complex functions by simple, sequential and quantitative functionalization of the active ester units and subsequent liberation of the amine functionalities.

Next we will demonstrate the application of the herein synthesized diblock copolymers for the surface modification of aldehyde-functionalized PS colloids (diameter = 4.9 μm; described in Scheme 2). The diblock copolymers, from now on termed PAEA-*b*-P(TEGA-*co*-BiotinTEGA) are remarkable in

Table 2. Selection of various diblock copolymers after post-polymerization modification of analogous PBocAEA-*b*-PPFPA

Polymer[a]	$M_{n,calc}$(Da)[b]	$M_{n,SEC}$ (Da)[c]	Đ
PBocAEA25-*b*-P(TEGA-co-BiotinTEGA)33	13,800	18,400	1.26
PBocAEA25-*b*-P(TEGA-co-BiotinTEGA)60	20,500	18,900	1.27
PBocAEA39-*b*-P(TEGA-co-BiotinTEGA)88	30,300	20,400	1.32

[a]Degree of polymerization determined by ^{1}H NMR (Biotin incorporation always 5 mol% compared to PFPA units). [b]Theoretical molecular weights based on weight fractions and absolute molecular weight of PBocAEA-CTA. [c]SEC in DMF (1 g/L LiBr) calibrated with PMMA standards.

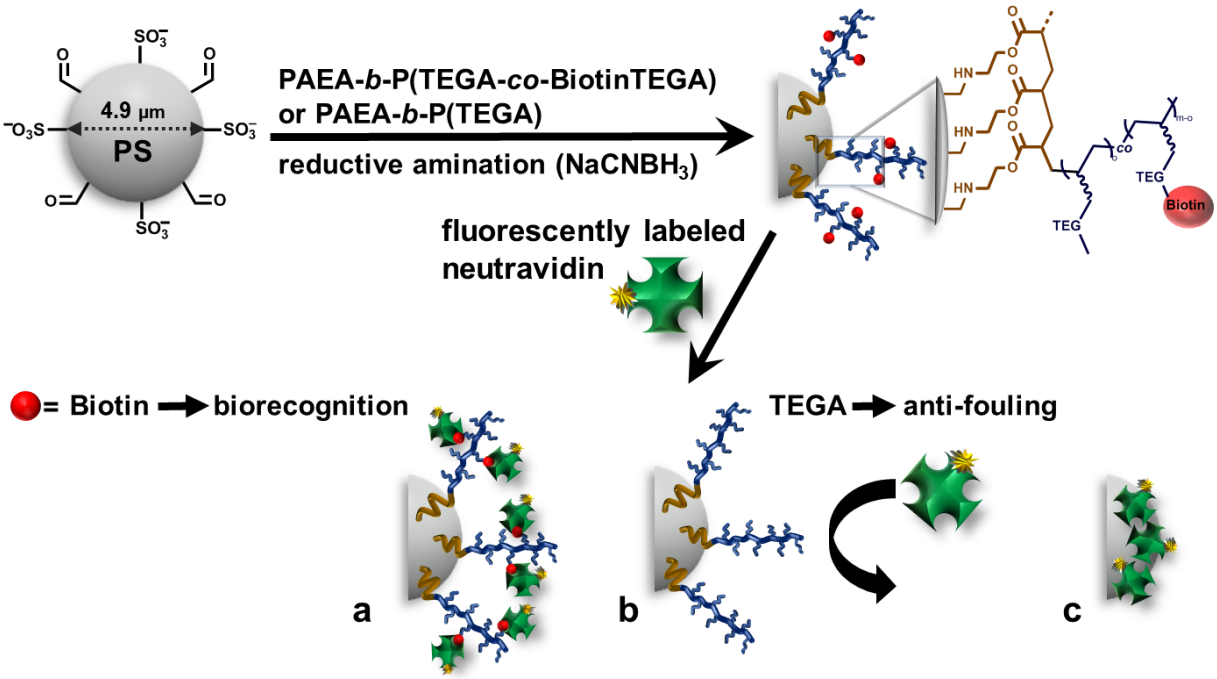

Scheme 2 Schematic representation of the covalent immobilization of the diblock copolymers with and without biotin functionality onto PS colloids carrying aldehyde groups. Reduction of intermediately formed Schiff base allows the formation of stable amine bonds. Coated (a+b) as well as uncoated ((c) as reference) PS microspheres are exposed to dye-labeled NAv.

terms of their functionality as they provide spatially separated multivalent attachment to the particle surface with a protein-repellent, branched TEG structure containing multivalent biorecognition units. Amine groups are particularly appealing for surface modification, as they have strong tendency for physisorption on a wide range of organic and inorganic substrates and provide simple ways for covalent attachment via (reductive) amination, nucleophilic substitution or Michael additions. We choose three different diblock copolymers (Table 2), differing in total molecular weight and in the relative weight fractions, to understand differences in the grafting density and biorecognition of neutravidin (NAv).

For theoretical rationalization, we can consider the process as an adsorption of block copolymers from non-selective solvents onto surfaces with an attraction of block A (PAEA) to the surface, yielding a swollen anchoring layer and a more diluted and extended buoy layer (PTEGA). Following the de Gennes formalism[71], Marquez and Joanny developed the scaling laws for describing the surface thickness and grafting density as a function of both blocks.[72] For very large adsorptive blocks, there is a continuous layer of block A with a low density of A-B junction points (grafting density). Upon decrease of the ratio of block A, the density increases and a tighter brush layer can be formed. For very small blocks of A, the layer tends to break up into a (semi)-dilute regime, while the non-adsorbing B chains still form a grafted layer. Obviously, very large A blocks are unfeasible and hence we focus on a range of block copolymers with larger amounts of the non-adsorbing B block, yet still providing tight multivalent adhesion and preventing break-up of the adsorptive layers into a semi-dilute patchwork. The crossover composition between both regimes is located at $N_A^{11/6} \approx N_B$ (N = degree of polymerization).[73] All our polymers conform to the continuous regime (Table 1). Therein, the grafting density, σ, is given by $\sigma \sim (N_A)^{-1}$, while the layer thickness scales with $L \sim N_A^{1/3} N_B a$ (a = monomer size, which for simplicity is assumed equal for A and B in the scaling theory). Hence, the grafting density is governed by the PAEA length, while the thickness of the adsorbed layers is more strongly dominated by the PTEGA block, thus overall molecular weight.

As experimental approach, we compare pristine particles, with particles containing covalently attached surface layers of biotin-free and biotinylated diblock copolymers. As a further comparison, we also include (i) a standard non-fouling coating which is formed by reductive amination of a monofunctional PEG-NH_2 (M_n = 2 kDa), as well as surface layers of (ii) pristine PAEA and (iii) two random copolymers P(AEA-co-(TEGA)) and P(AEA-co-TEGA-co-biotinTEGA) immobilized under equal conditions (see Supplementary Information for (ii) and (iii)). We measure the ζ-potential to elucidate the changes of the electrostatic potential from non-modified PS particles to modified particles. In all cases we find that the ζ-potential of the negatively charged PS colloids, stabilized by SO_3H groups, changes from – 41 mV to positive values in the range of 24 mV to 40 mV. This clearly indicates a successful binding and a similar surface charge for all particles after modification.

We analyze the extent of protein-repellency/non-fouling behavior and selective biorecognition (i) qualitatively by confocal fluorescence microscopy and (ii) quantitatively by

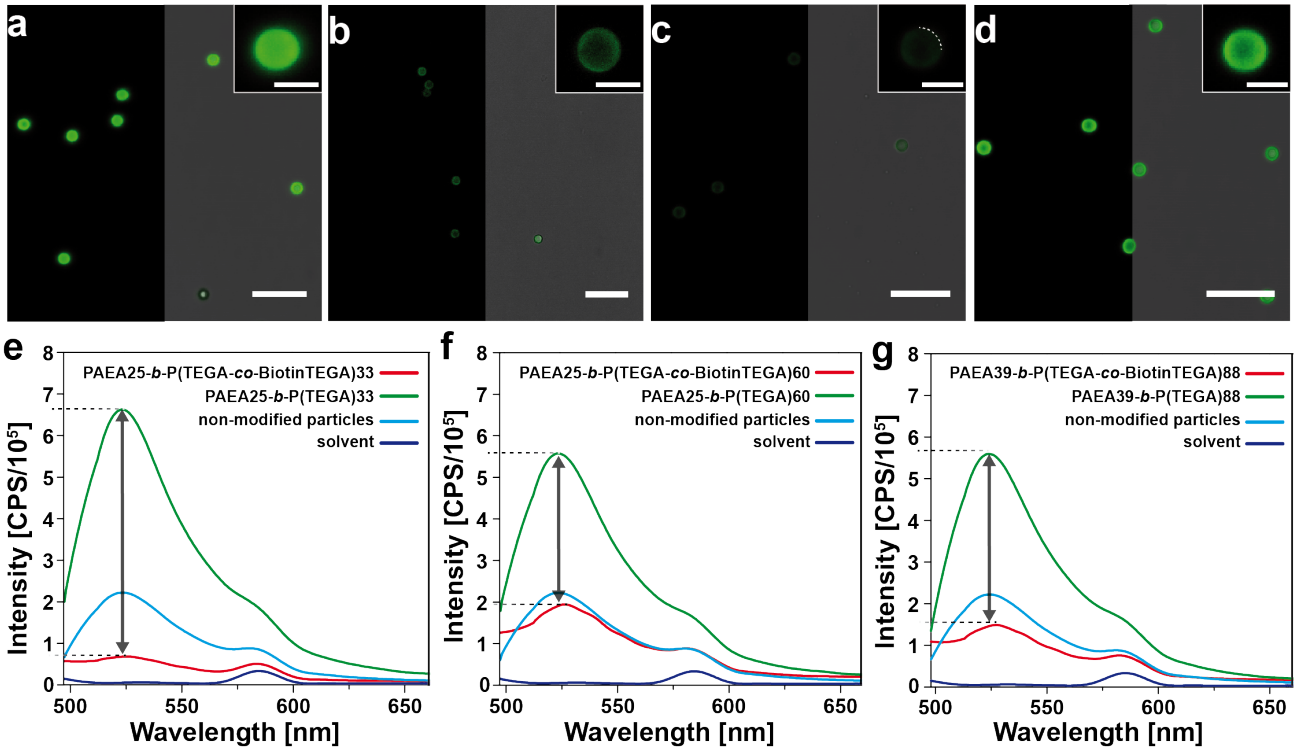

Figure 5 Homogeneous coating of PS colloids and protein repellency behavior with specific biorecognition using Biotin/Avidin complexation. (a-d) Confocal fluorescence micrographs of PS colloids were recorded after polymer immobilization and subsequent labeling with fluorescent NAv. Preparation and imaging conditions are equal for all samples. Fluorescence image **(a)** shows strong protein adsorption on pure PS colloids after mixing with fluorescent NAv. Fluorescence image **(b)** shows PS colloids after coating with commercial PEG-NH_2 (2 kDa) and subsequent treatment with fluorescent NAv. Fluorescence micrographs **(c,d)** of polymer-coated PS colloids without **(c)** and with biotin **(d)** clearly show the enhanced fluorescence due to biotin/NAv recognition in **(d)**, while non-fouling prevails in **(c)**. All scale bars are 25 µm (insets 5 µm). **(e-g)** Fluorescence emission spectra (λ_{ex} = 488 nm) of supernatant to monitor non-adsorbed fluorescent NAv in solution after addition to **(e)** PAEA25-*b*-P(TEGA-*co*-BiotinTEGA)33 and PAEA25-*b*-P(TEGA)33, **(f)** PAEA25-*b*-P(TEGA-*co*-BiotinTEGA)60 and PAEA25-*b*-P(TEGA)60 and **(g)** PAEA39-b-P(TEGA-co-BiotinTEGA)88 and PAEA39-b-P(TEGA)88 coated PS colloids, respectively. Non-modified colloids are shown for comparison. The black arrows and dashed lines are a guide to the eye.

fluorescence spectroscopy of the supernatant (to characterize non-bound proteins) after treating equal amounts of PS beads with an Oregon green labeled NAv. First, we will focus on the fluorescence microscopy recorded under standardized and equal conditions to allow for a visual comparison of the different samples. The pristine particles show strong non-specific adsorption/fouling of the fluorescently labeled NAv, as can be seen in the strongly fluorescent corona (Figure 5a).

A standard anti-fouling coating, after immobilization of linear and monofunctional PEG-NH_2 (Figure 5b), leads to a decrease of the fluorescence intensity in the rim region, corresponding to suppressed protein adsorption. However, exchanging the monovalent PEG-NH_2 (2 kDa) to our multivalent polymers with branched TEG structure leads to an almost complete disappearance of the fluorescence, confirming enhanced protein repellency (Figure 5c). This improvement is due to an increase in the packing density of TEG groups on the surface layer due to its branched architecture, which causes enhanced protein repellency arising from osmotic and steric repulsion.[74-77] This scenario can be inverted upon incorporation of small amounts of biotin into the branched TEG structure of the second block, which leads to successful and strong specific biorecognition toward the fluorescent NAv as evidenced in the appearance of strong fluorescence at the surface of the microsphere (Figure 5d).

As a further comparison, we find strong protein adsorption when the particles are coated with pristine PAEA homopolymer (Figure SI1a). More interestingly, even random copolymers P(PAEA-*co*-TEGA) and P(PAEA-*co*-TEGA-*co*-biotinTEGA) of a similar composition as the block copolymers show strong protein fouling, rather independent of whether biotin units are present or not (Figure SI1b,c). These results confirm the importance of the block-type architecture and spatial segregation of binding and functionality.

Further fluorescence spectroscopy of the supernatant to analyze the non-adsorbed proteins allows to reveal subtle differences between the various diblock copolymers and a more quantitative interpretation of the observations. Comparing the fluorescence spectra in Figure 5e-g, we find that the smallest polymer (PAEA25-*b*-P(TEGA-*co*-BiotinTEGA)33) (Figure 5e) leads to the lowest fluorescence intensity of the supernatant (compare red curves Figure 5e-g), which in turn corresponds to the highest specific recognition. Interestingly enough, the same polymer also shows the highest residual fluorescence (green curve, Figure 5e) if the biotin is omitted, hence corresponding to the most efficient protein repellency. Since this polymer

contains the overall smallest fraction of biotin units in the full polymer structures (Table 2 for composition), the highest extent of selective recognition and non-specific protein repellency must be related to the most efficient grafting-to reaction, leading to the highest grafting density of the polymer onto the PS beads. Due to the large size of the PS beads (as needed for visualization in the confocal microscope), it is however at this point not possible to fully quantify the mass fraction of immobilized diblock copolymer per surface area.

Conclusion

We established a straightforward strategy toward tailor-made diblock copolymers of mutually incompatible amine and active ester functionalities by consecutive RAFT polymerization, and demonstrated simple, stepwise, orthogonal and quantitative functionalization of both blocks. This is significant because it creates a new and versatile class of functional diblock copolymers that make very efficient use of the possibly most widely used ligation chemistry (amine/active ester). The active ester block can be readily functionalized with a broad range of functional amines, allowing to easily impart biological activity, as demonstrated for incorporating biotin units. The subsequent liberation of the amine functionalities enables a second set of orthogonal conjugations, for instance for covalent attachment via nucleophilic addition, or for non-covalent interactions and polyelectrolyte complexation to DNA. We exploited the amine moieties for tight immobilization onto PS colloids and demonstrated successful improvement in protein-repellent behavior, realizing both strong attachment to the particle surface and multivalent biorecognition to the surrounding media upon incorporation of biotin. Our comparison to random copolymers of similar composition also reveals that the spatial segregation of binding and biological functionalities using the block copolymer architecture allows superior performance in terms of non-selective protein-repellency and selective bioregnition.

Acknowledgements

We thank Anja Goldmann for measuring DMAc SEC and Björn Schulte for help with MALDI-ToF measurement. A.W. thanks M. Möller for continuous support. This work was performed in part at the Center for Chemical Polymer Technology CPT, which is supported by the EU and the federal state of North Rhine-Westphalia.

Notes and references

† Electronic Supplementary Information (ESI) available: Materials, instrumentation, monomer synthesis, synthesis of TEG-NH_2 and biotin-TEG-NH_2, synthesis of random copolymers, additional data on protein-repellency. See DOI: 10.1039/b000000x/

1. O. Altintas, A. P. Vogt, C. Barner-Kowollik and U. Tunca, *Polym. Chem.*, 2012, **3**, 34-45.
2. K. A. Günay, P. Théato and H.-A. Klok, *J. Polym. Sci., Part A: Polym. Chem.*, 2013, **51**, 1-28.
3. J. Brandt, K. K. Oehlenschlaeger, F. G. Schmidt, C. Barner-Kowollik and A. Lederer, *Adv. Mater.*, 2014, DOI:10.1002/adma.201400521.
4. W. Xi, T. F. Scott, C. J. Kloxin and C. N. Bowman, *Adv. Funct. Mater.*, 2014, **24**, 2572-2590.
5. R. Huisgen, *Proc. Chem. Soc.*, 1961, 357-396.
6. H. C. Kolb, M. G. Finn and K. B. Sharpless, *Angew. Chem. Int. Ed.*, 2001, **40**, 2004-2021.
7. D. Quemener, T. P. Davis, C. Barner-Kowollik and M. H. Stenzel, *Chem. Commun.*, 2006, 5051-5053.
8. A. S. Goldmann, D. Quémener, P.-E. Millard, T. P. Davis, M. H. Stenzel, C. Barner-Kowollik and A. H. E. Müller, *Polymer*, 2008, **49**, 2274-2281.
9. J. Nicolas, F. Bensaid, D. Desmaële, M. Grogna, C. Detrembleur, K. Andrieux and P. Couvreur, *Macromolecules*, 2008, **41**, 8418-8428.
10. S. Binauld, C. J. Hawker, E. Fleury and E. Drockenmuller, *Angew. Chem. Int. Ed.*, 2009, **48**, 6654-6658.
11. M. Müllner, A. Schallon, A. Walther, R. Freitag and A. H. E. Müller, *Biomacromolecules*, 2010, **11**, 390-396.
12. A. J. Inglis, P. Pierrat, T. Muller, S. Brase and C. Barner-Kowollik, *Soft Matter*, 2010, **6**, 82-84.
13. A. S. Goldmann, C. Schödel, A. Walther, J. Yuan, K. Loos and A. H. E. Müller, *Macromol. Rapid Commun.*, 2010, **31**, 1608-1615.
14. H. Zhao, W. Gu, E. Sterner, T. P. Russell, E. B. Coughlin and P. Theato, *Macromolecules*, 2011, **44**, 6433-6440.
15. C. J. Durr, S. G. J. Emmerling, P. Lederhose, A. Kaiser, S. Brandau, M. Klimpel and C. Barner-Kowollik, *Polym. Chem.*, 2012, **3**, 1048-1060.
16. C. Lang, K. Pahnke, C. Kiefer, A. S. Goldmann, P. W. Roesky and C. Barner-Kowollik, *Polym. Chem.*, 2013, **4**, 5456-5462.
17. T. T. T. N'Guyen, H. T. T. Duong, J. Basuki, V. Montembault, S. Pascual, C. Guibert, J. Fresnais, C. Boyer, M. R. Whittaker, T. P. Davis and L. Fontaine, *Angew. Chem. Int. Ed.*, 2013, **52**, 14152-14156.
18. E. Blasco, B. V. K. J. Schmidt, C. Barner-Kowollik, M. Pinol and L. Oriol, *Polym. Chem.*, 2013, **4**, 4506-4514.
19. C. Zhang, R. J. Macfarlane, K. L. Young, C. H. J. Choi, L. Hao, E. Auyeung, G. Liu, X. Zhou and C. A. Mirkin, *Nat. Mater.*, 2013, **12**, 741-746.
20. A. P. Vogt, J. De Winter, P. Krolla-Sidenstein, U. Geckle, O. Coulembier and C. Barner-Kowollik, *J. Mater. Chem. B*, 2014, **2**, 3578-3581.
21. R. Tiwari, D. Hönders, S. Schipmann, B. Schulte, P. Das, C. W. Pester, U. Klemradt and A. Walther, *Macromolecules*, 2014, **47**, 2257-2267.
22. K. L. Killops, L. M. Campos and C. J. Hawker, *J. Am. Chem. Soc.*, 2008, **130**, 5062-5064.
23. L. M. Campos, K. L. Killops, R. Sakai, J. M. J. Paulusse, D. Damiron, E. Drockenmuller, B. W. Messmore and C. J. Hawker, *Macromolecules*, 2008, **41**, 7063-7070.
24. A. S. Goldmann, A. Walther, L. Nebhani, R. Joso, D. Ernst, K. Loos, C. Barner-Kowollik, L. Barner and A. H. E. Müller, *Macromolecules*, 2009, **42**, 3707-3714.
25. G. Chen, S. Amajjahe and M. H. Stenzel, *Chem. Commun.*, 2009, 1198-1200.
26. M. J. Kade, D. J. Burke and C. J. Hawker, *J. Polym. Sci., Part A: Polym. Chem.*, 2010, **48**, 743-750.
27. N. Gupta, B. F. Lin, L. M. Campos, M. D. Dimitriou, S. T. Hikita, N. D. Treat, M. V. Tirrell, D. O. Clegg, E. J. Kramer and C. J. Hawker, *Nat. Chem.*, 2010, **2**, 138-145.
28. R. Tedja, A. H. Soeriyadi, M. R. Whittaker, M. Lim, C. Marquis, C. Boyer, T. P. Davis and R. Amal, *Polym. Chem.*, 2012, **3**, 2743-2751.
29. C. Schulz, S. Nowak, R. Fröhlich and B. J. Ravoo, *Small*, 2012, **8**, 569-577.
30. B. Schulte, C. A. Dannenberg, H. Keul and M. Möller, *J. Polym. Sci., Part A: Polym. Chem.*, 2013, **51**, 1243-1254.
31. M. A. Cole, K. C. Jankousky and C. N. Bowman, *Polym. Chem.*, 2013, **4**, 1167-1175.
32. P. Théato and R. Zentel, *Langmuir*, 1999, **16**, 1801-1805.
33. M. Eberhardt and P. Théato, *Macromol. Rapid Commun.*, 2005, **26**, 1488-1493.

34. J. Nicolas, E. Khoshdel and D. M. Haddleton, *Chem. Commun.*, 2007, 1722-1724.
35. P. Theato, *J. Polym. Sci., Part A: Polym. Chem.*, 2008, **46**, 6677-6687.
36. M. Chenal, C. Boursier, Y. Guillaneuf, M. Taverna, P. Couvreur and J. Nicolas, *Polym. Chem.*, 2011, **2**, 1523-1530.
37. S. Harrisson, P. Couvreur and J. Nicolas, *Macromolecules*, 2011, **44**, 9230-9238.
38. I. Singh, C. Wendeln, A. W. Clark, J. M. Cooper, B. J. Ravoo and G. A. Burley, *J. Am. Chem. Soc.*, 2013, **135**, 3449-3457.
39. H. Zhao, W. Gu, M. W. Thielke, E. Sterner, T. Tsai, T. P. Russell, E. B. Coughlin and P. Theato, *Macromolecules*, 2013, **46**, 5195-5201.
40. D. Seuyep, D. Szopinski, G. A. Luinstra and P. Theato, *Polym. Chem.*, 2014, DOI:10.1039/C1034PY00740A.
41. T. Pauloehrl, G. Delaittre, M. Bruns, M. Meißler, H. G. Börner, M. Bastmeyer and C. Barner-Kowollik, *Angew. Chem. Int. Ed.*, 2012, **51**, 9181-9184.
42. R. Novoa-Carballal and A. H. E. Muller, *Chem. Commun.*, 2012, **48**, 3781-3783.
43. R. Novoa-Carballal, A. Pfaff and A. H. E. Müller, *Polym. Chem.*, 2013, **4**, 2278-2285.
44. C. E. Hoyle, A. B. Lowe and C. N. Bowman, *Chem. Soc. Rev.*, 2010, **39**, 1355-1387.
45. A. H. Soeriyadi, G.-Z. Li, S. Slavin, M. W. Jones, C. M. Amos, C. R. Becer, M. R. Whittaker, D. M. Haddleton, C. Boyer and T. P. Davis, *Polym. Chem.*, 2011, **2**, 815-822.
46. W. Xi, M. Krieger, C. J. Kloxin and C. N. Bowman, *Chem. Commun.*, 2013, **49**, 4504-4506.
47. D. P. Nair, M. Podgórski, S. Chatani, T. Gong, W. Xi, C. R. Fenoli and C. N. Bowman, *Chem. Mater.*, 2013, **26**, 724-744.
48. T. Gruendling, K. K. Oehlenschlaeger, E. Frick, M. Glassner, C. Schmid and C. Barner-Kowollik, *Macromol. Rapid Commun.*, 2011, **32**, 807-812.
49. T. Tischer, A. S. Goldmann, K. Linkert, V. Trouillet, H. G. Börner and C. Barner-Kowollik, *Adv. Funct. Mater.*, 2012, **22**, 3853-3864.
50. K. K. Oehlenschlaeger, J. O. Mueller, N. B. Heine, M. Glassner, N. K. Guimard, G. Delaittre, F. G. Schmidt and C. Barner-Kowollik, *Angew. Chem. Int. Ed.*, 2013, **52**, 762-766.
51. C. M. Preuss, A. S. Goldmann, V. Trouillet, A. Walther and C. Barner-Kowollik, *Macromol. Rapid Commun.*, 2013, **34**, 640-644.
52. C. Rodriguez-Emmenegger, C. M. Preuss, B. Yameen, O. Pop-Georgievski, M. Bachmann, J. O. Müller, M. Bruns, A. S. Goldmann, M. Bastmeyer and C. Barner-Kowollik, *Adv. Mater.*, 2013, **25**, 6123-6127.
53. K. K. Oehlenschlaeger, J. O. Mueller, J. Brandt, S. Hilf, A. Lederer, M. Wilhelm, R. Graf, M. L. Coote, F. G. Schmidt and C. Barner-Kowollik, *Adv. Mater.*, 2014, **26**, 3561-3566.
54. T. Tischer, C. Rodriguez-Emmenegger, V. Trouillet, A. Welle, V. Schueler, J. O. Mueller, A. S. Goldmann, E. Brynda and C. Barner-Kowollik, *Adv. Mater.*, 2014, **26**, 4087-4092.
55. M. Langer, J. Brandt, A. Lederer, A. S. Goldmann, F. H. Schacher and C. Barner-Kowollik, *Polym. Chem.*, 2014.
56. J. Nicolas, V. S. Miguel, G. Mantovani and D. M. Haddleton, *Chem. Commun.*, 2006, 4697-4699.
57. C. Boyer, A. H. Soeriyadi, P. J. Roth, M. R. Whittaker and T. P. Davis, *Chem. Commun.*, 2011, **47**, 1318-1320.
58. P. J. Roth, F. D. Jochum, R. Zentel and P. Theato, *Biomacromolecules*, 2009, **11**, 238-244.
59. D. Kessler, P. J. Roth and P. Theato, *Langmuir*, 2009, **25**, 10068-10076.
60. F. D. Jochum, P. J. Roth, D. Kessler and P. Theato, *Biomacromolecules*, 2010, **11**, 2432-2439.
61. J. Nicolas, G. Mantovani and D. M. Haddleton, *Macromol. Rapid Commun.*, 2007, **28**, 1083-1111.
62. R. Tang, R. N. Palumbo, L. Nagarajan, E. Krogstad and C. Wang, *J. Control. Release*, 2010, **142**, 229-237.
63. M. Ma, F. Li, Z.-F. Yuan and R.-X. Zhuo, *Acta Biomater.*, 2010, **6**, 2658-2665.
64. M.-H. Dufresne and J.-C. Leroux, *Pharm. Res.*, 2004, **21**, 160-169.
65. W. Ji, D. Panus, R. N. Palumbo, R. Tang and C. Wang, *Biomacromolecules*, 2011, **12**, 4373-4385.
66. H. H. The, S. Pascual, V. Montembault, N. Casse and L. Fontaine, *Polym. Chem.*, 2014, DOI:10.1039/C1034PY00585F.
67. P. Kumar E.K, L. N. Feldborg, K. Almdal and T. L. Andresen, *Chem. Mater.*, 2013, **25**, 1496-1501.
68. C. Zhu, S. Jung, G. Si, R. Cheng, F. Meng, X. Zhu, T. G. Park and Z. Zhong, *J. Polym. Sci., Part A: Polym. Chem.*, 2010, **48**, 2869-2877.
69. M. Eberhardt, R. Mruk, R. Zentel and P. Théato, *Eur. Polym. J.*, 2005, **41**, 1569-1575.
70. E. Beyou, P. Chaumont, F. Chauvin, C. Devaux and N. Zydowicz, *Macromolecules*, 1998, **31**, 6828-6835.
71. P. G. de Gennes, *Adv. Colloid Interface Sci.*, 1987, **27**, 189-209.
72. C. M. Marques and J. F. Joanny, *Macromolecules*, 1989, **22**, 1454-1458.
73. C. Kuttner, A. Hanisch, H. Schmalz, M. Eder, H. Schlaad, I. Burgert and A. Fery, *ACS Appl. Mater. Interfaces*, 2013, **5**, 2469-2478.
74. J. Ladd, Z. Zhang, S. Chen, J. C. Hower and S. Jiang, *Biomacromolecules*, 2008, **9**, 1357-1361.
75. N.-J. Lin, H.-S. Yang, Y. Chang, K.-L. Tung, W.-H. Chen, H.-W. Cheng, S.-W. Hsiao, P. Aimar, K. Yamamoto and J.-Y. Lai, *Langmuir*, 2013, **29**, 10183-10193.
76. G. Gunkel, M. Weinhart, T. Becherer, R. Haag and W. T. S. Huck, *Biomacromolecules*, 2011, **12**, 4169-4172.
77. J. Groll, Z. Ademovic, T. Ameringer, D. Klee and M. Moeller, *Biomacromolecules*, 2005, **6**, 956-962.

Graphical Table of Contents Abstract

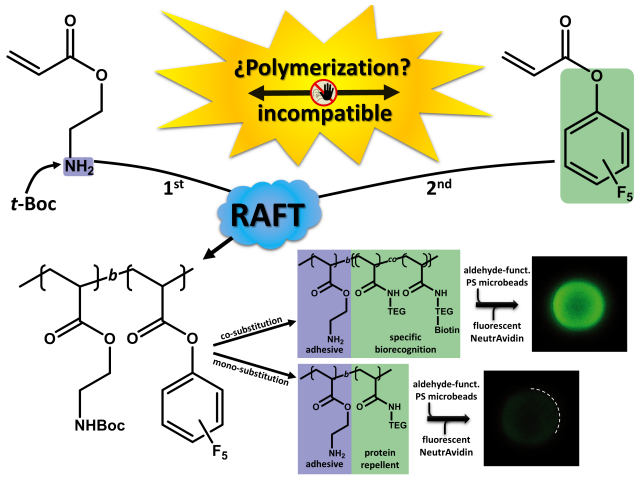

Short Abstract:

We present the facile synthesis and orthogonal functionalization of diblock copolymers consisting of two mutually incompatible segments, i.e. primary amines and activated esters, and demonstrate their use as surface modifiers on colloids to provide enhanced protein repellency and multivalent biorecognition.